TOOLS FOR CLASSIFICATION OF MINE-LIKE OBJECTS IN SYNTHETIC APERTURE SONAR IMAGES

J Engström SAAB Underwater Systems, Motala, Sweden
M Trieb SAAB Underwater Systems, Motala, Sweden
G. A. Shippey Dept. of Signals and Systems, Chalmers U. of Technology, Gothenburg, Sweden

1 INTRODUCTION

This paper presents some tools for use in the classification of Mine-Like Objects (MLOs) in Synthetic Aperture Sonar (SAS) imagery. The research is a first study on applying CAD/CAC to SAS data recorded by the SAAB Underwater Systems AUV62MR vehicle under the SAPPHIRES project.

The strategy presented here is that an object is detected at an earlier operational stage, either with the same or a different sonar. Then a SAS image is generated covering the immediate neighbourhood of the object. In this smaller area image the highlight and shadow regions are segmented and features afterwards extracted. Eventually these features are used for classification purposes. This paper deals with the segmentation and the feature extraction part. These two parts of the system have been handled separately in order to avoid interdependency between them.

A number of different approaches to image segmentation can be found in the literature, with thresholding being perhaps the most basic. For segmentation of sonar images, more sophisticated approaches can be considered, for example the Markov Random Field approach discussed in[1,2,3]. Local statistics for segmentation purpose are discussed in[4] where the Mean – Standard deviation plane is used. This paper presents a segmentation scheme using a region growing[5] approach based on local statistics, using the Mean – Standard deviation plane. Features that might be used to discriminate man-made objects from natural ones and also features describing size and shape of objects are evaluated on experimental SAS images. The test images used in this paper can be found in section 7 where they have been quantized and adjusted for visual reasons. However all processing has been carried out on 64-bits float data from the image reconstruction algorithm.

The data was recorded using a 1.5 m long, 48-element, receiver array. The sonar operates at 100 kHz with bandwidths up to 30 kHz. With an element width of 30 mm, the theoretical limit for along-track resolution is 15 mm. However the resolution for the test images is 6.25 x 6.25 cm. The transmitter-array is also multi-element, in order to allow vertical beam-steering for multi-path elimination. Since the AUV62MR has the necessary computing resources for SAS processing within the vehicle, a working CAD/CAC system could also be installed in the vehicle. Thereafter it would only be necessary to transmit the SAS image surrounding each object, together with CAD/CAC parameters back to the command station to decide on countermeasures.

2 SEGMENTATION USING A REGION GROWING APPROACH

2.1 Theory

Beside local statistics, the segmentation scheme uses *a priori* knowledge,

- A true highlight region from an interesting object lies within a certain size bracket
- A true shadow region from an interesting object has approximately the same along track dimension as corresponding highlight.

- A true shadow region has across-track dimensions larger than a certain value
- A true highlight region is followed by a true shadow region.

The statistic measures used here are local mean and local standard deviation. For an image, X, and a local window, size (i x j), these are given by Equations 1 and 2 respectively.

$$X_{MEAN}(m,n) = \frac{\sum_{k=-(i-1)/2}^{(i-1)/2} \sum_{l=-(j-1)/2}^{(j-1)/2} X(m+k,n+l)}{ij} \quad (1)$$

$$X_{SD}(m,n) = \sqrt{\frac{\sum_{k=-(i-1)/2}^{(i-1)/2} \sum_{l=-(j-1)/2}^{(j-1)/2} (X(m+k,n+l))^2 - ijX_{MEAN}}{ij}} \quad (2)$$

It is discussed in[4] and in the attached references that highlight pixels have high local mean but standard deviation with varying characteristics, while shadow pixels have low local mean and standard deviation. The local statistic for background pixels varies depending of the complexity of the seabed. For flat sediment without protruding small rocks, background pixels have the same characteristic as shadow pixels, low local mean and standard deviation, and it might be possible to segment highlights by thresholding. For more complex seabed structures, a different solution is needed. Fig. 1 shows the Mean – Standard deviation plane for Test Image 3 from Fig. 6. As can be seen, background pixels are distributed across the plane. Hence it is not possible to segment all highlight pixels by thresholding. By choosing the red line shown in the figure as a threshold for local-mean, highlight seed pixels are found for use in the Region Growing Algorithm. The threshold, T_1, is set by a linear combination, Eq. 3, of the mean value for all pixels in the original image, X, size (MxN), and the maximum value in the local mean image, X_{MEAN}.

$$T_1 = (1 - A_1) * \max(X_{MEAN}) + A_1 * \left(\frac{\sum_{m \in M} \sum_{n \in N} x(m,n)}{MN} \right) \quad (3)$$

With a structured background, for example where small rocks are scattered on the seabed, background pixels might still be falsely initiated as highlight pixels. This risk is addressed later in the processing.

In the next step, neighbouring pixels are incorporated in the region if their greyscale value is higher than T_2, a new lower threshold, defined by a linear combination, Eq. 4, of mean-value of pixels already classified as highlight and mean-value of all pixels in the image.

$$T_2 = (1 - A_2) * \frac{\sum_{m \in M} \sum_{n \in N} x(m,n) \subset HIGHLIGHT}{N_{HIGHLIGHT}} + A_2 * \left(\frac{\sum_{m \in M} \sum_{n \in N} x(m,n)}{MN} \right) \quad (4)$$

where $N_{HIGHLIGHT}$ is the number of highlight pixels in the Image

When no more pixels can be incorporated, holes and pixels not already classified as highlight but surrounded only by highlight pixels are filled. Regions failing the first *a priori* criterion are then removed.

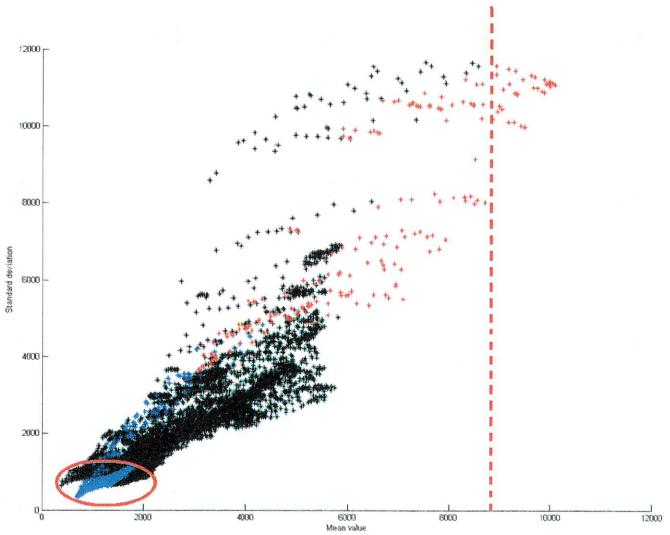

Fig. 1 **The Mean – Standard deviation plane for Test Image 3 from Fig. 6. Red points are for highlight pixels, blue for shadow and black for background. The red line marks the threshold for finding seed pixels. The red ellipse marks pixels with typical shadow characteristics, i.e. low mean-value and standard deviation.**

Seed pixels for the shadow regions, one region for each highlight region, are found by defining a window, SW, in the area behind the highlight. These are pixels where the local mean and local standard deviation are below the thresholds T_3, T_4 (Eq. 5 and Eq. 6), respectively. The size of SW is set by the along- track size of the highlight region and the minimum expected width of the shadow, across-track.

$$T_3 = (1 - A_3) * \min(X_{MEAN}(SW)) + A_3 * \left(\frac{\sum_{m \in M_{SW}} \sum_{n \in N_{SW}} x_{MEAN}(m,n)}{M_{SW} N_{SW}} \right) \quad \textbf{(5)}$$

$$T_4 = (1 - A_4) * \min(X_{SD}(SW)) + A_4 * \left(\frac{\sum_{m \in M_{SW}} \sum_{n \in N_{SW}} x_{SD}(m,n)}{M_{SW} N_{SW}} \right) \quad \textbf{(6)}$$

For the shadow-growing step, two more thresholds T_5 and T_6 are defined, again using linear combinations (Eq. 7, 8). These relax the requirements for a pixel neighbouring a shadow pixel to be classified as shadow. Growing of the shadow region is accepted if a neighbouring pixel has local standard deviation and mean below T_5, T_6 respectively. Growth outside the previous defined window

is now permitted. However to fulfil the second *a priori* criterion, growth beyond the along-track dimension of the highlight is forbidden.

$$T_5 = (1 - A_5) * \frac{\sum_{m \in M} \sum_{n \in N} x_{SD}(m,n) \subset SHADOW}{N_{SHADOW}} + A_5 * \left(\frac{\sum_{m \in M} \sum_{n \in N} x_{SD}(m,n)}{MN} \right) \quad (7)$$

$$T_6 = (1 - A_6) * \frac{\sum_{m \in M} \sum_{n \in N} x_{MEAN}(m,n) \subset SHADOW}{N_{SHADOW}} + A_6 * \left(\frac{\sum_{m \in M} \sum_{n \in N} x_{MEAN}(m,n)}{MN} \right) \quad (8)$$

Where N_{SHADOW} is the number of shadow pixels in the image.

After shadow growth, holes are filled in the same way as for the highlight. Finally, regions that don't fulfil all *a prior* criteria are removed.

2.2 Segmentation of Experimental SAS Images

Fig. 2 shows the result of the above segmentation scheme, step by step, for Test Image 4 from Fig. 7.

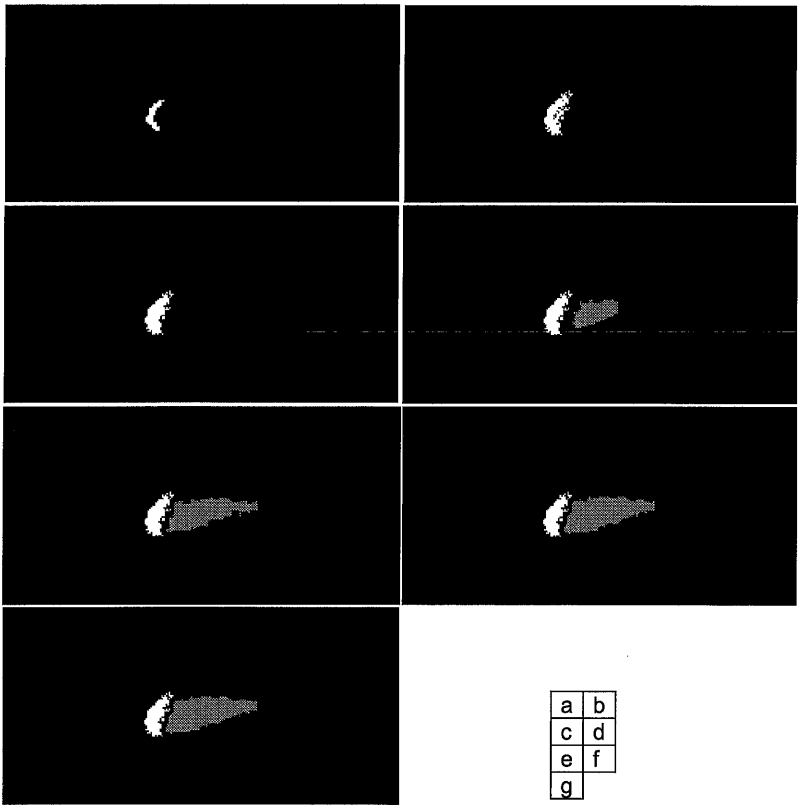

Fig. 2 **Segmentation of Test Image 4, Fig. 7. a) highlight seed pixels b) after highlight growing c) final highlight region d) shadow seed pixels e) after 1st shadow growing step f) After 2nd shadow growing step g) Final segmentation**

In section 7, the scheme has been applied to all test images using the same parameter configuration. The results are good except for Test Image 2, Fig. 5, where a region of background pixels has been merged with the highlight region. A special parameter selection is needed to segment the highlight region from the background successfully. Parameters are currently chosen by trial and error, but in future a way to determine these parameters from the image statistics is needed.

Fig. 3 shows the comparison between the manual segmentation and the segmentation obtained by the above scheme for Test Images 4 and 7.

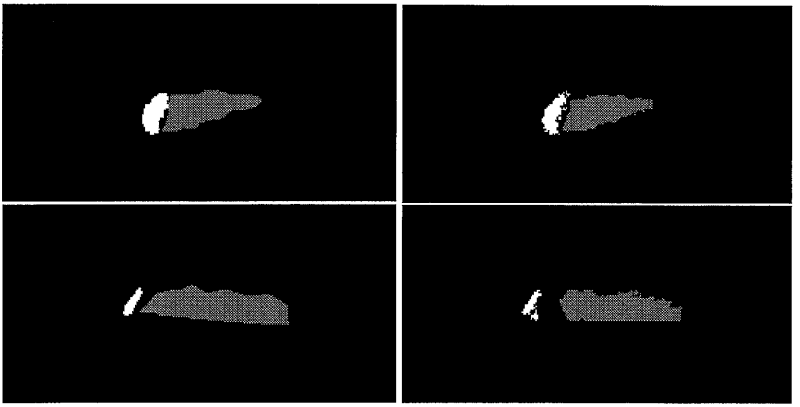

Fig. 3 **Comparison between manual segmentation and computer segmentation for Test Images 4 and 7. The left images are manually segmented.**

The difference for the shadow region in Test Image 7 is worth noticing. In the computer segmented version, the shadow has a straight line that is not present in the manual segmented image. This artificial boundary line is due to the second *a priori* criterion.

3 FEATURE EXTRACTION

3.1 Object Smoothness Features

Objects protruding from the seabed return a stronger echo towards the sonar. Natural objects tend to have rougher surfaces than mines and other man-made objects. A rough surface scatters the energy in all direction while an effectively smooth surface, with roughness dimensions less than the sonar wavelength, reflects the energy with a peak in the specular (mirror-like) direction[6]. The sonar can receive specular reflections when the plane of the surface is normal to the direction of the transmitted pulse. Results are presented here using three different features to characterise the above: mean-value of highlight intensity, peak intensity, and standard deviation for all highlight pixels divided with mean value.

3.2 Shape Features

Object shape is important for determining its nature. Shape features discussed here are size, parallel lines, right-angled corners and rectangularity.

An object which is unexpectedly small or large is unlikely to be a mine, so can be ignored, or at least given less priority in the mine counter-measure part of the system. Since the exact size of many mines is known[7] an accurate size would also suggest the type of mine. To be able to see the complete object boundary, steeper elevation angles are needed than were used in these experiments. Therefore only the size of the boundary facing the sonar can be estimated. The width of an object, where are the highlight stretches across the whole object, is given by Eq.9

$$w = l\rho \quad [m] \qquad (9)$$

where l is the length, in pixels, of the highlight region for the object and ρ is the image resolution in $[m/pixel]$. For a highlight parallel to the track of the vessel, l is given by the elongation in the along-track dimension. For a highlight skew to the track, for example Test Image 7 in Fig.10, l is estimated after applying the Hotelling/ Kauren-Loeve transform.

The height of an object is given by Eq. 10.

$$h = \frac{ShadowLength * Altitude}{ShadowRange} \quad [m] \qquad \textbf{(10)}$$

ShadowLength is the length of the shadow. Altitude is the height of the sonar platform above the seabed, so Altitude/Shadowrange is the tangent of the insonification elevation angle. An important characteristic of SAS is that shadows become eroded by rotation of the insonification angle in azimuth, so h can only be an approximation to the true height.

Man-made objects often have sharp edges and symmetric shapes. Many mines also have shapes resembling basic geometric shapes such as spheres, boxes, cylinders and truncated cones. If any of these features can be inferred from the sonar image, it suggests that the object is man-made. However no conclusion can be drawn from their absence.

Straight edges in the shape of the highlight and/or shadow region indicate a sharp edge in the object. If two edges are parallel, or form a right-angle, a man-made object is indicated. In very high-resolution SAS-images, highlight details can be seen, so edges in the highlight region might also be of interest. However none of these early test images had such characteristics so this possibility was not investigated.

Linearities in the image were found using the Hough Transform[5], where the accumulation matrix is thresholded based on region size. Since lines $s = x\cos\theta + y\sin\theta$ in the transform are represented by the point $[s,\theta]$, two lines i, j are parallel if $\theta_i = \theta_j$. They form a right-angle if $\left|\theta_i - \theta_j\right| = 90°$.

Rectangularity[5] of a region is a measure defined by Eq.11

$$R = \frac{A}{ab} \qquad \textbf{(11)}$$

where A is the area of the region and a is the maximum span in any direction, while b is the span at right-angles to that direction. This rectangularity parameter, R, is measured in both highlight and shadow sections. A highlight or shadow shaped like a perfect rectangle is probably generated by a man-made object. However the appearance of the shadow region depends on the insonification angle, so high rectangularity is more interesting in the highlight region.

4 FEATURES EXTRACTED FROM EXPERIMENTAL IMAGES

The purpose here is to assess the value of the different features for mine classification, so the highlight and shadow regions were segmented manually.

Table 1 shows the result of the features describing the smoothness of object surface discussed above for 7 objects found in data from the SAPPHIRES project. Intensities are given with a nominal scale factor.

Test Image	Object	Peak Intensity	Mean Intensity	$\frac{Std.Deviation}{Mean}$	Range [m]
1	Anchor	6,22	1,69	0.72	38
2	Torpedo	5,73	1,68	0.58	64
3	Rock	7,08	1,11	0.93	53
4	Rock	5,65	1,01	0.80	39
5	Rock	7,97	0,84	1.33	40
6	Mine	4,76	1,57	0.82	50
7	Mine	7,59	1,98	0.65	56

Table 1 **Features describing smoothness of the object surface. The results are for the test images shown in Section 7 after manual segmentation**

Attenuation with range is already compensated in the image reconstruction algorithm, so no further correction is applied. Of the above features, mean intensity looks the most useful as a classification feature, while standard deviation/mean is promising, but insufficient in itself for confident discrimination.

Im.	Object	Corners		Parallel lines		Rectangularity		Longest line [m]		Highlight size [m]	Obj. height [m]
		H.	S.	H.	S.	High.	Shad.	H.	S.		
1	Anchor	0	0	0	0	0.6493	0.5155	0.5	1.62	1.10	0.5
		0		0		0.6664		0.5		1.01	
2	Torpedo	0	0	0	0	0.7897	0.7166	0.69	1.44	2.96	1.1
3	Rock	0	0	1	0	0.7218	0.7243	0.50	1.31	1.30	0.5
4	Rock	0	0	0	0	0.7133	0.6841	0.56	1.56	1.84	0.8
5	Rock	0	3	1	0	0.7771	0.6420	0.44	0.75	1.13	0.2
6	Mine	0	0	0	0	0.8407	0.8395	0.50	4.31	0.92	0.9
7	Mine	0	0	0	0	0.8222	0.7819	0.44	1.25	1.23	0.8

Table 2 **Features describing object shape. The results are for manually segmented test images in section 7. Since Test Image 1 has two highlight regions, two values are given. The mines in Test Images 6 and 7 are box-shaped with approximate size 1.0x0.7x0.7 [m].**

Table 2 shows the results for the shape features. As discussed in section 3.2, object size is a useful feature, when it can be estimated accurately. Further tests, including dependency on segmentation, are needed to assess the accuracy of size estimation. More accurate estimation might also be possible when the bathymetric part of the AUV 62 MR system is implemented.
Regarding the other shape features, rectangularity shows promise as a indicator for man-made objects, while the line-based features (longest line, parallel lines and corners) need improved thresholding of the accumulation matrix in the Hough transform.

5 CONCLUSIONS AND FURTHER WORK

The segmentation scheme presented here is based on a standard image analysis algorithm, region growing using local statistics. The method works well on the small set of test image tested here, but will almost certainly need development for use with a wider test set. One concern is the large number of parameters used to set the limits. More extensive testing is needed to find a generally applicable set of parameter values. Preliminary testing has also been carried using the Markov Random Field[1,2,3] approach, where parameters are determined from the statistics of the image itself. A similar approach should be investigated for Region Growing. Another possible way to improve the result is to use higher order statistics discussed in[8] and normalized standard deviation.

Regarding MLO classification features, the tentative conclusions which can be drawn from this small test set is that mean intensity and standard deviation/mean might be helpful. The Size Features are probably only useful when mines have already been found in the area, and the search can be narrowed to finding similar ones while rectangularity might be possible to use for indicating man-made objects.

The Test Images shown here were obtained at an early stage of system testing, so improved spatial resolution can be expected in the future. If so, then the methods and features discussed here should be even more useful.

6 ACKNOWLEDGMENT

The help of many at SAAB Underwater Systems who supplied information and image data under considerable time pressure is gratefully acknowledged.

7 TEST IMAGES

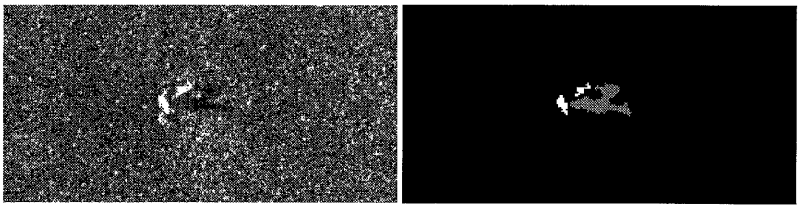

Fig. 4 Test image 1. Anchor at range ≈ 38 m, altitude ≈ 9.6 m
a) original image **b) computer segmented image, using same parameter set for all test images**

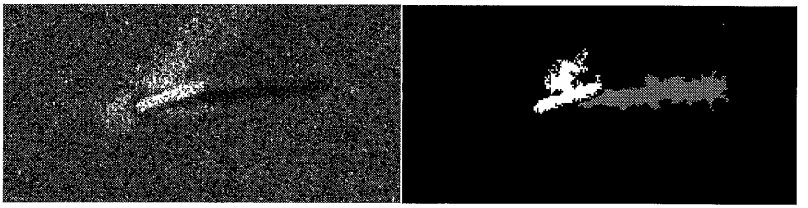

Fig. 5 Test Image 2. Torpedo at range ≈ 64 m, altitude ≈ 16.9 m
a) original image **b) computer segmented image**

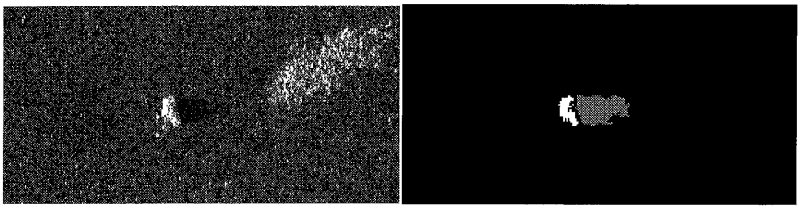

Fig. 6 Test Image 3. Rock at range ≈ 53 m, altitude ≈ 10.9 m
a) original image b) computer segmented image

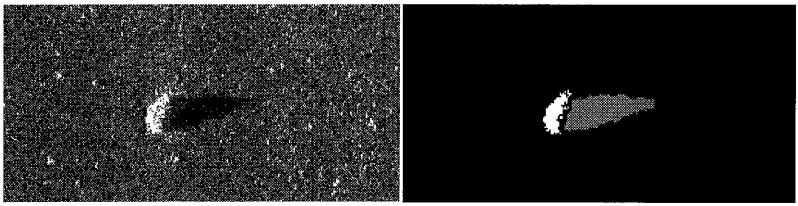

Fig. 7 Test Image 4. Rock at range ≈ 39 m, altitude ≈ 9.0 m
a) original image b) computer segmented image

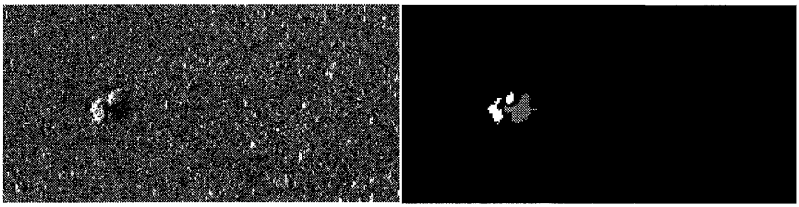

Fig. 8 Test Image 5. Rock at range ≈ 40 m, altitude ≈ 8.4 m
a) original image b) computer segmented image

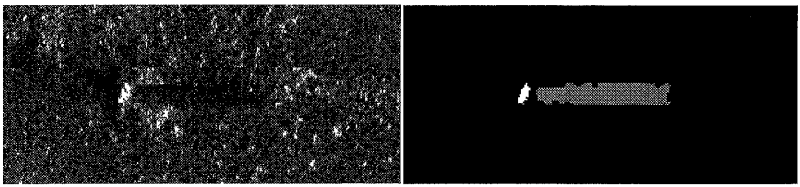

Fig. 9 Test Image 6. Mine at range ≈ 50 m, altitude ≈ 8.5 m
a) original image b) computer segmented image

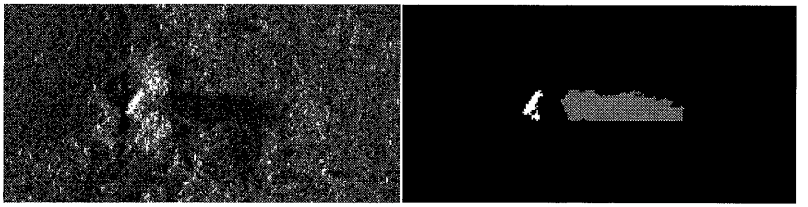

Fig. 10 Test Image 7. Mine at range ≈ 56 m, altitude ≈ 8.5 m
a) original image b) computer segmented image

8 REFERENCES

1. M. Mignotte, C. Collet, P. Pérez and P. Bouthemy, "Three-Class Markovian Segmentation of High-Resolution Sonar Images," Computer Vision and Image Understanding Vol.76, No. 3, December, pp. 191-204, 1999.
2. M. Mignotte, C. Collet, P. Pérez and P. Bouthemy. *Unsupervised segmentation applied on sonar images.* In Proc. International Workshop EMMCVPR'97: Energy Minimisation Methods in Computer Vision and Pattern Recognition, volume LNCS 1223, pages 491--506, Venice, Italy, May 1997. Springer-verlag.
3. S. Reed, Y. Petillot, and J. Bell, "An Automatic Approach to the Detection and Extraction of Mine Features in Sidescan Sonar" *IEEE Journal of oceanic engineering* Vol.28, No. 1, January 2003.
4. F.Maussang, J. Chanussot, and A. Hétet, "Automated Segmentation of SAS Images using the Mean – Standard Deviation Plane for the Detection of Underwater Mines," in *Proceedings of MTS/IEEE Oceans'03 conference*, San Diego, California, USA, September 2003, pp. 2155 – 2160.
5. M. Sonka, V. Hlavac, R.Boyle,"Image Processing, Analysis and Machine Vision". Brooks/Cole Publishing Company. IBSN 0-534-95393-X, 1999.
6. A.D. Waite, "SONAR for Practising Engineers, "John Wiley & Sons Ltd. ISBN 0471497509, 2002
7. "Oceanography and Mine Warfare", Ocean Studies Board, National Research Council. ISBN 978-0-30906798-0. 2000. Http://books.nap.edu/openbook.php?isbn=0309067987
8. F. Maussang, J. Chanussot, and A. Hétet, "On the use of higher order statistics in SAS imagery," in *Proceedings of IEEE International Conference on Acoustics, Speech and Signal Processing (ICASSP '04)*, vol. 5, pp. 269–272, Montreal, Quebec, Canada, May 2004.